Title	Applied analysis to DNA knot by topological invariants (Mathematical Aspects for nonlinear problems related to Life-phenomena)
Author(s)	Yoshino, Takashi; Onishi, Isamu
Citation	数理解析研究所講究録 (2008), 1616: 181-194
Issue Date	2008-10
URL	http://hdl.handle.net/2433/140144
Right	
Type	Departmental Bulletin Paper
Textversion	publisher

数理解析研究所講究録
第1616巻 2008年 181-194

Applied analysis to DNA knot by topological invariants
位相不変量を用いたDNA結び目に対する応用解析

Takashi Yoshino and Isamu Onishi (Hiroshima University)
吉野　貴史、大西　勇　（広島大学　大学院理学研究科　数理分子生命理学専攻）

Contents

1 Introduction

1.1 Topological Structures of a DNA

The structure of DNA is a double helix, much like a ladder that is twisted into a spiral shape. In 1953 the double-helix structure of a DNA was proposed by J. D. Watson and F. H. Crick with technique to build a molecular model. The double helix is the ideal model that J. D. Watson and F. H. Crick arrived at from many studies about a DNA and seven next important characteristics are emphasized in the structure.

1. The double helix is formed by two polynucleotide.
2. A purine and a pyrimidine ring orient it in the inside of the double helix.
3. The base in complementary relations is bound by hydrogen bond.
4. There is 10.4 base pair per spiral 1 round per minute.
5. As for two polynucleotide of the double helix, a direction is reverse (reverse parallel) each .
6. Double helix has two kinds of grooves, the major groove and the minor groove.
7. The double helix is clockwise twining (right handed).

When a double-stranded DNA of the double-helix structure is twisted more or it is untied, the double helix is more twisted as a whole. These are called the supercoiled structure (a positively supercoiled DNA is the former and a negatively supercoiled DNA is the latter, respectively).

The ringed supercoiled DNA closed by covalent bond has "the twist" and "the writhe". "The twist" is the spiral number of revolutions that one chain surrounds the chain of the other, that is the number of times that one chain completely coils the chain of the other. "The twist" in a right-handed spiral is defined as plus. "The writhe" is a number that the double strand coils oneself or the double strand is coiled cylindrically like the cord of the telephone. The total value of "the twist" and "the writhe" cannot be changed unless we cut off the DNA. As an enzyme changing topological structure of the DNA, we take the transpososome and the topoisomerase for an example.

1.2 Transpososome

The transpososome is a complex of the transposon and the transposase. The transposon is the base sequence which can perform a transposition on the genome in a cell. An enzyme called transposase, which transposon oneself encodes, is necessary for transposon DNA to perform transposition.

The transposon has the reverse repetitive sequences on the end and the transposase recognizes this arrangement and cuts a transposon from a DNA arrangement. Therefore it is necessary for transposase to cut each DNA chain at each end of the transposon. The cutting happens in a linkup with the host DNA adjacent to a transposon. The transposase cuts the DNA to leave the reverse repetitive sequences (or the part) in the place where a transposon originally was in. After a transposon was cut, the end of the transposon DNA that is the end that transposase cut first attacks the DNA phosphodiester bond of a new insertion part. This DNA domain is called the target DNA. Because the transpososome was formed, two ends of the transposon DNA attack two chains of the same target DNA. As a result of attack, the transposon DNA is bound by the covalent bond to the DNA of the target part.

Although the transpososome changes topological structures of the DNA, different products is expressed by the global structure of the DNA [1]. In the two plasmid substrates pSPIn and pSPDir, the loxP sites (the targets for the Cre protein) are in inverted (head to head) and direct (head to tail) orientations, respectively (Fig.1) . They divide each plasmid into two domains shown in red and blue. Recombination mediated by the Cre tetramer would yield a DNA inversion product with pSPIn and a pair of deletion circles with pSPDir.

In a general case, if n interdomainal supercoil nodes (n being odd) were trapped in the unknown synapse, inversion by Cre would result in a DNA knot with n crossings (Upper area of Fig.1) . Notice

that an odd number of trapped nodes would arrange the loxP sites of pSPIn in antiparallel alignment. For the Cre deletion reaction in pSPDir, an additional node ($|n| + 1 = even$) has to be introduced for the antiparallel arrangement of the loxP sites (Lower area of Fig.1) . The products of deletion would be a pair of catenated circles linked by ($|n| + 1$) crossings. These nodes are preserved in the recombination products, and report on the DNA topology within the synapse. The location of the loxP sites in these plasmids is such that the hybrid synapse has very little chance of accidentally acquiring interdomainal nodes, depending on the loxP orientation.

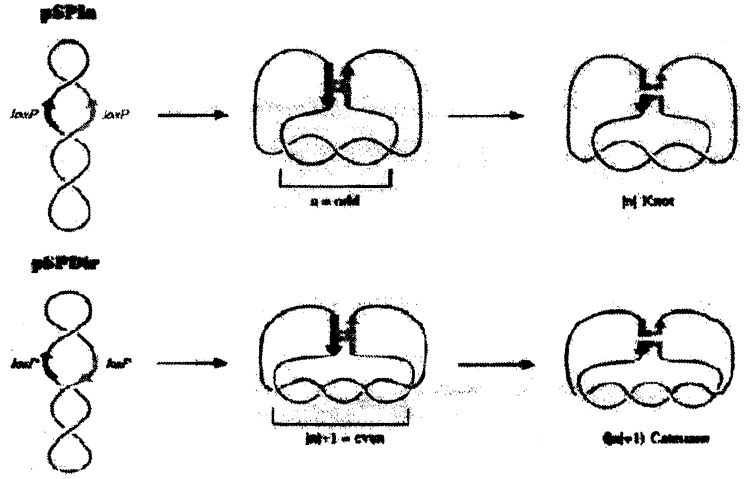

Fig. 1 Cre Recombination from a Preassembled Synapse

1.3 Topoisomerase

The topoisomerase is the enzyme which can change structures of the DNA by cutting the single strand or the double strand of the DNA temporarily.

The topoisomerase has two types. Type I topoisomerases cut the single strand of the DNA temporarily and connect it again after dipping the other single strand. Type II topoisomerases cut the double strand temporarily and close after dipping another double strand which is not cut.

Both a prokaryote and organism with a nucleus have type I and II topoisomerase which can remove the supercoiled structure from the DNA. Prokaryotes possess two structurally similar type II topoisomerases, Gyrase and Topo IV, which differ in their function. Gyrase generates negative supercoils, but Topo IV relaxes positive supercoils. In addition, it has reported that Gyrase is strongly bound with DNA, but Topo IV is weak [2].

The global structure of DNA strongly ties to the expression pattern of DNA by the property of Topo IV and Gyrase, since the different DNA structure tends to produce different DNA modification even under the same local condition. For example, when Gyrase was added to the positively supercoiled DNA, Gyrase unties DNA since Gyrase generates a negatively supercoils, but when Gyrase was added to the negatively supercoiled DNA, Gyrase twists DNA more. Thus, the global structure of the DNA is important for an enzyme.

It is known that the global topological structures of DNA tend to affect the expression of transcripts. DNA is affected by other nucleic acids and enzymes in the process of DNA transcription. The global structure of DNA strongly ties to the expression pattern of DNA, since the different DNA structure tends to produce different DNA modification even under the same local condition. Then it has been reported that the global topological structures of DNA influences expression of transcripts by performing various topological changes in genetic recombination [1]. In this paper we describe the topological structures of

DNA in a phage.

1.4 Structures of a phage

A phage is a virus which infects bacteria. It is well known that It is well known that it has tails and a regular icosahedral head(see Fig.2). A phage is the simplest system to study a basic process of life. The genome is small generally and the genome reproduce only after invading a host cell (a bacteria cell). Then a gene is expressed. A genome tends to be rearranged while infection.

Because the system is simple, a phage was used very well at the molecular biological dawn. Actually, a phage was indispensable for the development of this field. The system is also most suitable for a study of the DNA replication, the gene expression and basic structures of the recombination today. Furthermore, a phage is important as a vector of the DNA recombination, and it is used to examine the activity inducting variation of various compounds.

Phages usually pack genomes (generally, DNA) to a mantle consisting of subunits of the protein. A subunit has a one making head structure (packing genomes) and a one making tail structure. The phage particle is glued to the outside of the bacteria host cell with a tail and injects a phage genome to a cell. Because each phage glues to a specific molecule (usually, protein) in the cell surface, only a cell having a coping acceptor is infected with a phage.

A phage has a double-stranded DNA controlling a genetic information in the head. The linear DNA packed in the head of phages forms various types of knots. As the part of knots, Fig.3 shows knots 0_1, 3_1, 4_1, 5_1, 5_2, 6_1, 6_2, 6_3, 7_1, 7_2, 7_3, 7_4, 7_5, 7_6 and 7_7.

It is the important step of the DNA studies to investigate the fractions of various types of knots and clarify the reasons of the phenomena.

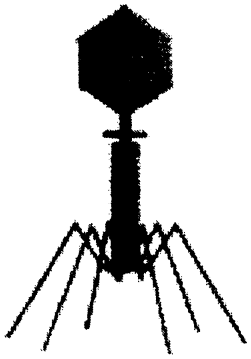

Fig. 2 A bacteriophage

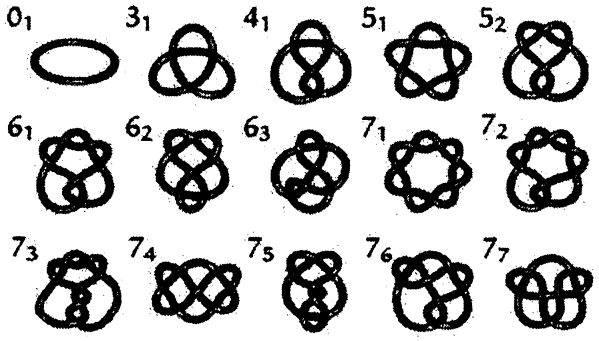

Fig. 3 The prime knots having below 7 crossing

1.5 Results of biological experiments

The DNA inside the phage was examined types of knots which is made inside the phage and the probability by J. Arsuaga et. al. [3]. First, purified DNA was analyzed by two-dimensional gel electrophoresis. By gel electrophoresis, we can distinguish some knot types with the number of the same crossing number. To the direction of I of Fig.4, DNA samples were run at $0.8V/cm$ for $40h$ at room temperature. After a 90° rotation of the gel, the direction of II of Fig.4 was run in the same electrophoresis buffer at $3.4V/cm$ for $4h$ at room temperature. This gel electrophoresis segregated the linear DNA molecules and segregated knots with six and more crossings to two groups. Knot populations of low crossing number are showed in Fig.5. The number of the right in Fig.5 is indicated the crossing number.

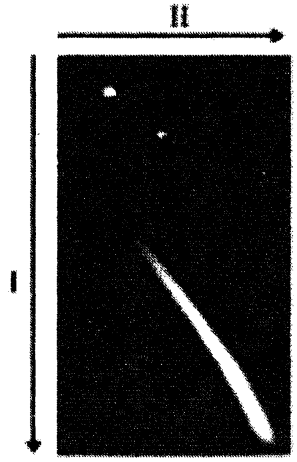

Fig. 4 The result of gel electrophoresis by J. Arsuaga et. al. [3]

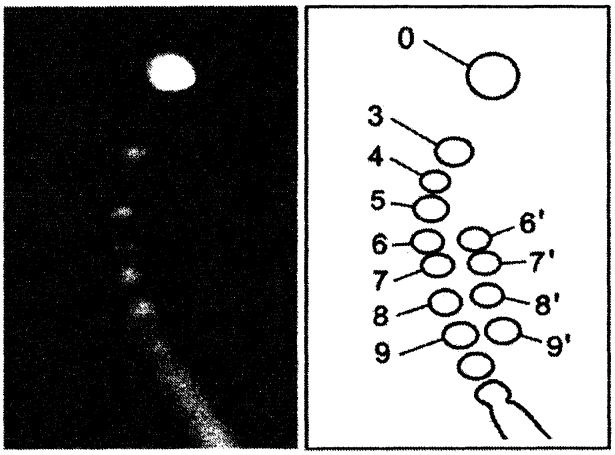

Fig. 5 The enlarged picture of Knot populations of low crossing number in Fig.4

Next, the projection obtained by this experiment was compared with the projection of known knot types to examine the knots corresponding DNA knots separated by electrophoresis (see Fig.6). The gel velocity at low voltage of individual knot populations resolved by two dimensional electrophoresis (Right of Fig.6) is compared with the gel velocity at low voltage of twist knots (3_1, 4_1, 5_2, 6_1 and 7_2) of a $10-kb$ nicked plasmid (Center of Fig.6) and with known relative migration distances of some knot types (Left of Fig.6). By this comparison, some knot types of each population are distinguished. In addition to the unambiguous knots 3_1 and 4_1, the knot population of five crossings matched the migration of the knot 5_1. The knot 5_2 appeared to be negligible or absent. The knot population of seven crossings matched the migration of the torus knot 7_1 rather than the twist knot 7_2. Yet, we cannot identify this gel band as the knot 7_1, because other possible knot types of seven crossings cannot be excluded.

Then, several indicators led us to believe that the second arch of the gel ($6'\sim9'$ of Fig.5) consists of mainly composite knots (see Def.2.6 in Chapter 2). First, the arch starts at knot populations containing six crossings, and no composite knots of fewer than six crossings exist. Second, the population of six crossings matched the migration at low voltage of the granny knot (composite of a 3_1 plus a 3_1, indicated as $3_1\#3_1$) , although the square knot (the other possible composite of six crossings, $3_1\#-3_1$) cannot be excluded. Third, consistent with the low amount of 4_1 knots, the size of the seven-crossing subpopulation is also reduced; thus, any composite seven-crossing knot is $3_1\#4_1$ (or $-3_1\#4_1$). The increased gel velocity at high voltage of composite knots relative to prime knots (see Def.2.5 in Chapter 2) of the same crossing number likely reflects distinct flexibility properties of the composites during electrophoresis.

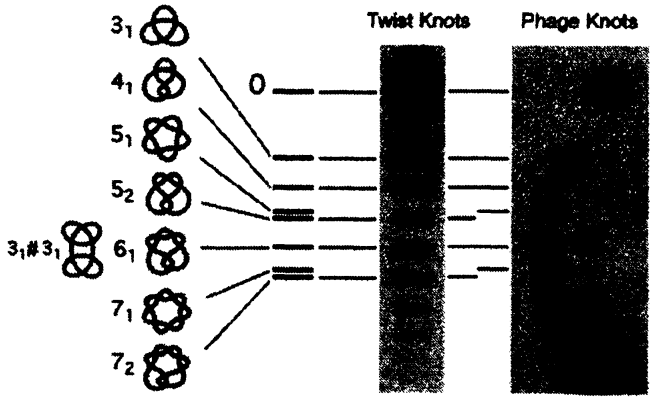

Fig. 6 Upper area of the gel picture showing knot populations of low crossing number

Densitometer readings confirmed the apparent scarcity of the knot of four crossings (knot 4_1) relative to the other knot populations in the main arch of the gel. Fig.7 shows the results of the fractions of knots 3_1, 4_1, 5_1 and 5_2 by biological experiments. However, the scarcity of the knot 4_1 relative to the knot of three crossings (knot 3_1) and to other knot populations is enhanced if we make the correction for DNA molecules plausibly knotted outside the viral capsid. In such a case, one can predict that 38% of the total number of observed 3_1 knots and 75% of the observed 4_1 knots are formed by random knotting in free solution.

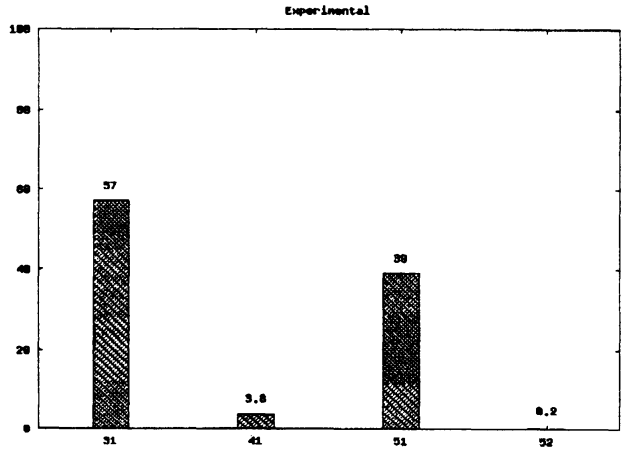

Fig. 7 The results of the fractions of knots 3_1, 4_1, 5_1 and 5_2 by biological experiments [3]

1.6 Outline of this study

To study the geometry of the DNA inside the phage, we simulated the fractions of the various types of knots and compared to those of biological experiments.

First, we simulated under the assumption that DNA knots inside the phage were generated at random. With Mersenne Twister we randomly made the knot topology having n crossings ($n = 3, 4, \cdots, 8$). This process was repeated $1,000,000$ times to obtain $1,000,000$ knots. Then we classified these knots with the invariant for the knot and estimated the fractions of the knots. These trials were repeated 100 times

and we considered the mean value of all trials as the conclusive fractions of the above-mentioned types of knots.

Next, we examined "the writhe value" Wr at each crossing. After eliminating matrices having the small value of the total amount $\sum Wr$, we performed the same simulation on the remaining matrices. The fractions of the knots 3_1, 4_1, 5_1 and 5_2 after considering "the writhe value" were similar to the biological results.

2 Preparations from Topology

Def. 2.1 (Alexander matrix) Let G be a group and let $\alpha : G \to G/[G,G]$ be the Abel map. The image $A(G,\alpha)$ of Jacobian by the Abel map α is called **Alexander matrix** of G.

Def. 2.2 (Alexander polynomial) The g. c. d. of determinant of $(n-1)\times(n-1)$ submatrix of $n\times n$ Alexander matrix is called **Alexander polynomial**.

Def. 2.3 (Trivial knot) Let $K \subset S^3$ be a knot. If there exists $K \subset S^2$ for a two-dimensional sphere $S^2 \subset S^3$, then K is called **the trivial knot**.

Def. 2.4 (Connected sum of knot) Let $K_1 \subset S^3$, $K_2 \subset S^3$ be knots and let $B_1 = S^3 - intN(x_1)$, $B_2 = S^3 - intN(x_2)$ for points $x_1 \in K_1$, $x_2 \in K_2$. If we set $S_i = \partial B_i \quad (i = 1,2)$, then S_i is a two-dimensional sphere and $K_i \cap S_i$ is a one-dimensional sphere in S_i.

Then we identify S_1 with S_2 and identify $K_1 \cap S_1$ with $K_2 \cap S_2$ by a homeomorphic mapping $(S_1, K_1 \cap S_1) \to (S_2, K_2 \cap S_2)$, and we connect $(B_1, K_1 \cap B_1)$ and $(B_2, K_2 \cap B_2)$.

The obtained knot $K \subset S^3$ is called **the connected sum** of K_1 and K_2, we use the notation $K_1 \sharp K_2$. Conversely, it is called that K is decomposed K_1 and K_2.

Def. 2.5 (Prime knot) For the arbitrary decomposition $K = K_1 \sharp K_2$ of the knot K, if at least one of K_1 or K_2 is the trivial knot, then K is called **the prime knot**. However, we define that the trivial knot is not the prime knot.

Def. 2.6 (Composite knot) If there exists a decomposition $K = K_1 \sharp K_2$ of the knot K such that K_1 and K_2 is the non-trivial knot which is not prime, then K is called **the composite knot**.

Def. 2.7 (Skein relation) Let t be the nonzero complex number and let L_+, L_- and L_0 be three knots that only one part crosses like a Fig.8 and the other part is totally same.

Then

$$tV_{L_+}(t) - t^{-1}V_{L_-}(t) = -(t^{1/2} - t^{-1/2})V_{L_0}(t)$$

is called **Skein relation**.

Fig. 8 Three knots L_+, L_- and L_0

Def. 2.8 (Jones polynomial) The polynomial $V_L(t)$ such that Skein relation hold is called **Jones polynomial**. However, Jones polynomial of the trivial knot of one component defines 1.

Def. 2.9 (Bracket polynomial) The polynomial $< D >$ of one variable A obtained by applying next three rules to the link diagram D is called **Bracket polynomial**:

(i) $< U >= 1$;
(ii) $< DU >= -(A^2 + A^{-2}) < D >$;
(iii) $<$  $>= A <$  $> + A^{-1} <$  $>$;
$<$  $>= A <$  $> + A^{-1} <$  $>$;

where U is a trivial knot, DU is an union with a trivial knot and we apply (iii) locally at each crossing of the link diagram.

Then for the link diagram D of an arbitrary knot L with the direction, Jones polynomial $V_L(t)$ has a relation with Bracket polynomial $< D >$ by

$$V_L(A^{-4}) = (-A^3)^{-\omega(D)} < D >,$$

where $\omega(D)$ is the sum of "the writhe value" at each crossing of the link diagram D (see Section 3.1.1).

It is known that the Alexander polynomial and Jones polynomial, which are the invariant for knots, is effectively used for the classification of knots based on the topology. We can classify all prime knots having below 8 crossing by a combination of the value of $\Delta(-2)$ and $\Delta(-3)$ when we use Alexander polynomial $\Delta(t)$. Then we can distinguish the mirror images of knots and knots having more crossings when we use Jones polynomial.

3 Simulations

3.1 Alexander polynomial

3.1.1 Elements of Alexander matrix

We shall project the knot on a place along an arbitrarily chosen axis, while drawing breaks at the crossing points in the part of the curve that lies below. Now the projection of the knot amounts to the set of segments of curves, which are called the generators. Let us fix arbitrarily the direction of passage of the generators and number them, having selected arbitrarily the first generator. The crossing that separates the kth and $(k+1)$th generators will be called the kth crossing. The crossings are of two types (see Fig.9). The writhe value Wr is $Wr = -1$ at type I crossing and $Wr = 1$ at type II crossing. The elements of Alexander matrix $A(t)$ are defined as follows [4].

1. When $i = k$ or $i = k+1$, independently of the type of crossing: $a_{kk} = -1$, $a_{kk+1} = 1$.
2. When $i \neq k$, $i \neq k+1$, for a type I crossing: $a_{kk} = 1$, $a_{kk+1} = -t$, $a_{ki} = t - 1$.
   for a type II crossing: $a_{kk} = -t$, $a_{kk+1} = 1$, $a_{ki} = t - 1$.
3. All the elements except a_{kk}, a_{kk+1} and a_{ki} are zero.

Here k is the number of crossing and i is the number of the overpassing generator. Then these relationships hold for all $k = 1, \cdots, n$ under the condition of the substitution $n + 1 \rightarrow 1$.

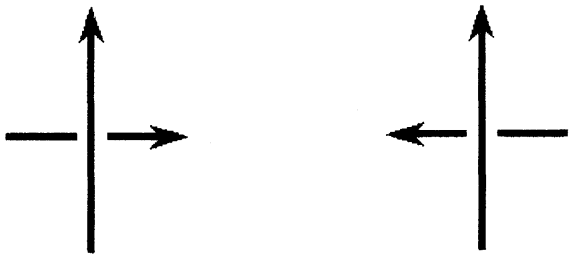

Fig. 9 The type I crossing (left) and the type II crossing (right)

3.1.2 Generation of Alexander matrix

First, we fix the dimension n of the Alexander matrix from 3~8 with Mersenne Twister at random. Second, we fix the element a_{kk} $(k = 1, 2, \cdots, n)$ of $n \times n$ matrix $A(-2), A(-3)$ $(n = 3, 4, \cdots, 8)$ substituted $t = -2, t = -3$ with Mersenne Twister as to satisfy above list. When $i \neq k$ and $i \neq k+1$, we take i with Mersenne Twister at random (i must not take k and $k+1$). This work is repeated from $k = 1$ to $k = n$ and we make the $n \times n$ matrix corresponding to the random knot.

3.1.3 Reidemeister moves

By Reidemeister moves, we untie the part which can untie of the knot. Reidemeister moves I, II (Fig.10) are the next operation [4].

I. If the kth row contains only two nonzero elements $a_{kk} = -1$ and $a_{kk+1} = 1$, then we should add the column k to the column $k+1$. Then we delete the kth column and the kth row and renumber the rows and column afresh.
II. If in two adjacent rows of the matrix having the numbers k and $k+1$ elements having the value $t-1$ lie in a single column and elements equal to $t-1$ are lacking in the $(k+1)$th column, then we should add the kth column to the $(k+2)$th, and then delete the kth and $(k+1)$th rows and columns and renumber all the rows and columns afresh.

The above list I and II correspond Reidemeister moves I and II, respectively.

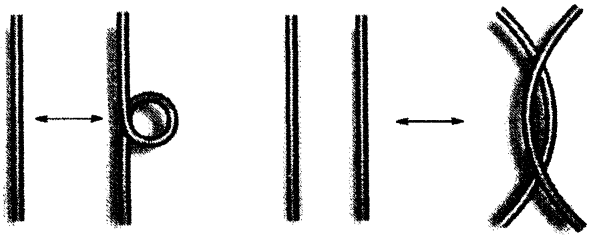

Fig. 10 Reidemeister moves I (left), II (right)

3.1.4 Classification of knots

We estimate the value $\Delta(-2)$, $\Delta(-3)$ of the determinant of the $(n-1) \times (n-1)$ submatrix and classify knots by the combination of the value of the determinant. Here, we removed all rows and columns from the first row and column to the nth row and column one by one. Then we treated as a knot when the value $\Delta(-2)$, $\Delta(-3)$ of all determinants was equal or different $\pm\, 2^m$ times, $\pm\, 3^m$ times (m is an

integer).

3.1.5 Reliability of the simulation

We gave 1,000,000 matrices at random and counted the number which generated each knot and estimated the fractions. These trials were repeated 100 times and we considered the mean value of all trials as the conclusive fractions of the types of knots.

3.1.6 Addition of "the writhe"

After the simulation of the random matrices, we employed "the writhe value" in the simulation. we examined "the writhe value Wr" at each crossing. After eliminating matrices having the small value of the total amount $\sum Wr$, we performed the same simulation on the remaining matrices.

3.2 Jones polynomial

3.2.1 Recurrent algorithm of Bracket polynomial

Because we can find Jones polynomial from Bracket polynomial if we find "the writhe value" of the knot, we constitute algorithm by Bracket polynomial [5].

For an arbitrary link diagram D, we paint with two colors of the black and white so that adjacent domains do not become the same color. Here, infinite domain is the white. Next, we choose one point in each black domain. If two black domains are adjacent, we link the point that we chose of each domain and we establish the sign of the edge based on Fig.11. Thus, the plane graph S with the sign is obtained.

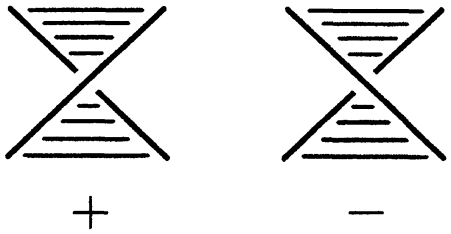

Fig. 11 The sign in two adjacent black domains

We define that $S\backslash e$ is the graph which deleted the edge e from the graph S and S/e is the graph which contracted the edge e from S (that is the edge e is condensed and the top of both ends correspond one point). Then we define that the loop is the edge where both ends are the same tops and the bridge is the edge where the connected component of the graph increases one when the edge is deleted.

It is known that the contraction / deletion formula of the edge holds for graph S with the sign. For example, when the edge linking two adjacent black domains is positive, the operation which tie two black domains and the operation which divide two black domains is equivalent to the contraction and the deletion, respectively.

$$< S >= A < S/e > +A^{-1} < S\backslash e >$$

Then when the edge e is the positive bridge, $S\backslash e$ is disconnectedness (that is the number of the component of the knot corresponding to $S\backslash e$ increases one), but $S\backslash e$ and S/e is the isomorphism, and the following relations hold between them.

$$< S\backslash e >= (-A^2 - A^{-2}) < S/e >$$

Therefore, they hold the following relations when the edge e is the positive bridge.

$$\begin{aligned} < S > &= A < S/e > +A^{-1} < S\backslash e > \\ &= -A^{-3} < S\backslash e > \end{aligned}$$

It is similar in the case of the negative bridge or the loop too, therefore they hold the following recurrence relations.

$$< S >= \begin{cases} -A^{-3} < S/e > & \text{if } e \text{ is the positive bridge} \\ -A^{3} < S/e > & \text{if } e \text{ is the negative bridge} \\ -A^{3} < S\backslash e > & \text{if } e \text{ is the positive loop} \\ -A^{-3} < S\backslash e > & \text{if } e \text{ is the negative loop} \\ A < S/e > +A^{-1} < S\backslash e > & \text{if } e \text{ is positive (otherwise)} \\ A < S\backslash e > +A^{-1} < S/e > & \text{if } e \text{ is negative (otherwise)} \end{cases}$$

Then when S consists of one edge (the positive bridge C^+, the negative bridge C^-, the positive loop L^+, the negative loop L^-), Bracket polynomials hold the following relations.

$$< C^+ >= -A^{-3},\ < C^- >= -A^{3},\ < L^+ >= -A^{3},\ < L^- >= -A^{-3}$$

Furthermore, when the edge set of S is the empty, Bracket polynomial has 1 from 2.9 (i).

3.2.2 Generation of the random plane graph with the sign

First, we fix the number of the top from 2~8 with Mersenne Twister at random and also fix the number of the edge from 3~8 at random. Next, we choose tops linked each edges at random and give the sign at random. Thus, we generate the random plane graph with the sign.

3.2.3 Classification of knots

We substitute 2 for variable A of Bracket polynomial and evaluate the recurrence algorithm of Bracket polynomial for the given graph. Then we classify knots by the value which was finally obtained. Here, because we considered the difference of the value of "the writhe value" of the knot, we also treated as the knot when the value which was finally obtained was different $(-2)^{3m}$ times (m is an integer).

3.2.4 Reliability of the simulation

We gave 1,000,000 matrices at random and counted the number which generated each knot and estimated the fractions. These trials were repeated 100 times and we considered the mean value of all trials as the conclusive fractions of the types of knots.

4 Results and Disucussion

4.1 Comparison of the results by Alexander polynomial and those by Jones polynomial

When knots were generated at random, Fig.12 shows the results by Alexander polynomial and Fig.13 shows those by Jones polynomial ($*$ in Fig.13 represents the mirror images of knots). In both results, the fraction of the knot 3_1 was the highest, the fractions of 4_1 was the second highest, 5_2 was the third and 5_1 was the fourth. In knots having 6 crossing, the fraction of the knot 6_2 was the highest, the fractions of 6_3 was the second and 6_1 was the third. Furthermore, by the results by Jones polynomial, the fractions of the knot and the mirror images of the knot has about the same fractions at each knot.

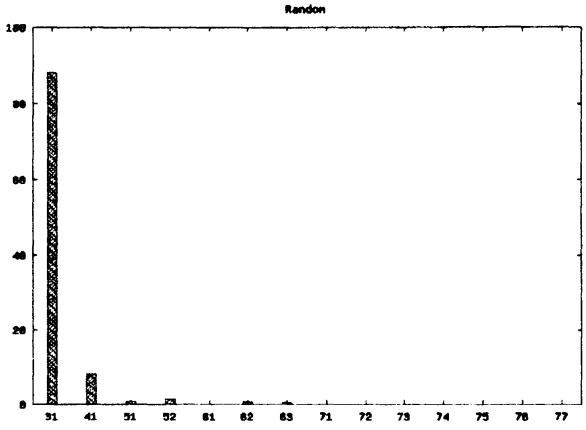

Fig. 12 Fractions distinguished knots generated at random by Alexander polynomial

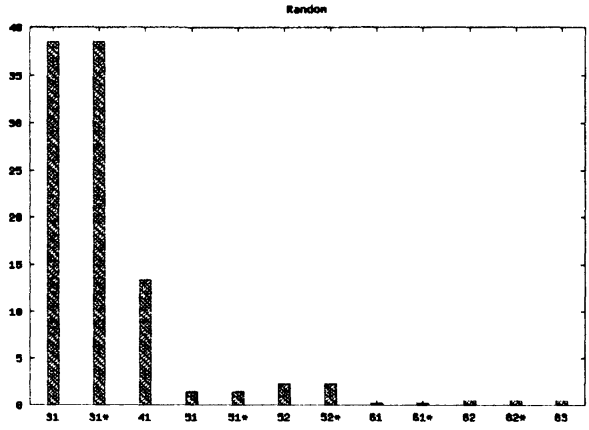

Fig. 13 Fractions distinguished knots generated at random by Jones polynomial

4.2 Comparison of the results of the simulation and those of biological experiments

About knots 3_1, 4_1, 5_1 and 5_2, we compare the results of the simulation by Alexander polynomial with the results of biological experiments. The fraction of knot types that emerged in biological experiments conducted by J. Arsuaga et. al. [3] is shown in Fig.14. In the biological experiments the fraction of the knot 3_1 was the highest and the fractions of 5_1 was the second highest, while 4_1 and 5_2 were low (Fig.14). In contrast, the fraction of knots that were computationally generated at random (Fig.15) was very different from the results of biological experiments. In Fig.15, the abundance of 4_1 was higher than 5_1 and 5_2.

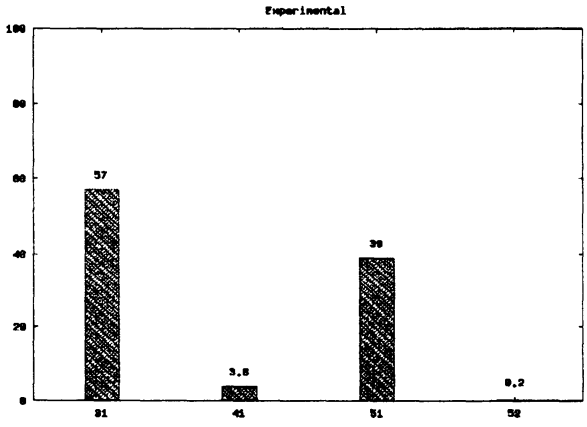

Fig. 14 The results of biological experiments by J. Arsuaga et. al. [3]

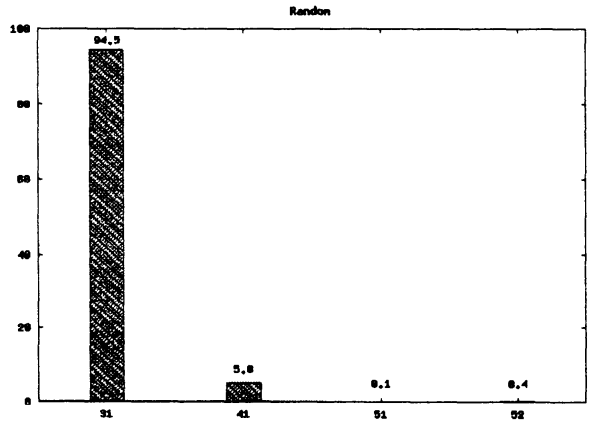

Fig. 15 Fractions of the knots 3_1, 4_1, 5_1 and 5_2 generated at random

However, employing "the writhe value" in the simulation changed the results. The fractions of the knots 3_1, 4_1, 5_1 and 5_2 after considering "the writhe value" were similar to the biological results (Fig.17).

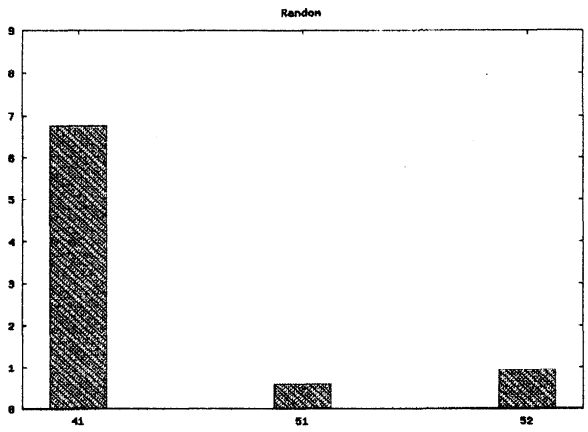

Fig. 16 Fractions of the knots 4_1, 5_1 and 5_2 generated at random

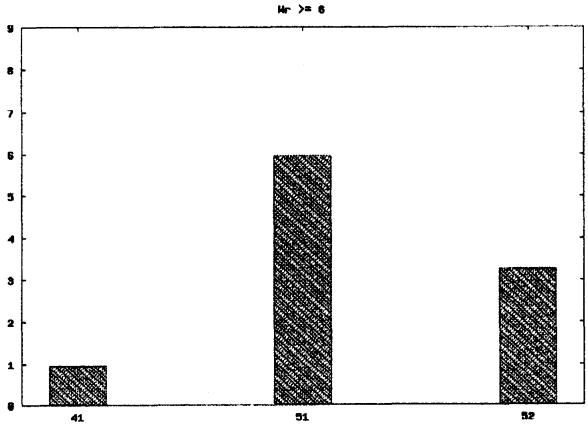

Fig. 17 Fractions of the knots 4_1, 5_1 and 5_2 after examining "the writhe value"

4.3 Disucussion and Future problems

We conclude that DNA knots inside the phage are not generated at random and they would have some bias being related to "the writhe value".

In future, we will devise simulation methods for distinguishing knots having more crossings. Furthermore, we will introduce the algorithm considering "the writhe value" into simulation by Jones polynomial.

References

[1] S. Pathania, M. Jayaram and R. M. Harshey, *Path of DNA within the Mu Transpososome: Transposase Interactions Bridging Two Mu Ends and the Enhancer Trap Five DNA Supercoils* , Cell, **Vol.109,** (2002), 425–436.

[2] G. Charvin, T. R. Strick, D. Bensimon and V. Croquette, *Topoisomerase IV Bends and Overtwists DNA upon Binding,* Biophysical Journal, **Vol.89,** (2005), 384–392.

[3] J. Arsuaga, M. Vazquez, P. McGuirk, S. Trigueros, D. W. Sumners and J. Roca, *DNA knots reveal a chiral organization of DNA in phage capsids,* PNAS, **Vol.102,** (2005), 9165–9169.

[4] M. D. Frank-Kamenetskii and A. V. Vologodskii, *Topological aspects of the physics of polymers: The theory and its biophysical applications,* Sov.Phys.-Usp.(Engl.Transl.), **Vol.24,** (1981), 679–696.

[5] K. Sekine, H. Imai and K. Imai, *Computation of the Jones Polynomial,* Transactions of JSIAM, **Vol.8,** (1998), 341–354.